First Results from LHC 13 TeV Run and other Recent Production Measurements

Svende Braun
on behalf of the LHCb collaboration
Heidelberg University, Physikalisches Institut

Hadron 2015, Newport News
September 13-18, 2015

UNIVERSITÄT
HEIDELBERG
ZUKUNFT
SEIT 1386

Measurements covered in this talk

1. Recent Production Measurements from Run-I
   - Λ_b^0 and $\overline{B}^0$ production at $\sqrt{s} = 7$ and $8\ \mathrm{TeV}$- arXiv:1509.00292
   - Υ production at $\sqrt{s} = 7$ and $8\ \mathrm{TeV}$- arXiv:1509.02372

2. First Results from LHC Run-II
   - J/ψ production cross-sections at $\sqrt{s} = 13\,\mathrm{TeV}$ - arXiv:1509.00771
   - prompt charm production cross-sections at $\sqrt{s} = 13\,\mathrm{TeV}$ - LHCb-PAPER-2015-041

Motivation

$\rightarrow$ important input to MC model tuning
$\rightarrow$ direct test of production mechanism $\rightarrow$ test of QCD
$\rightarrow$ LHCb performs measurements in unique kinematic region: $2 < \eta < 5$

LHCb Detector

JINST 3 S08005 (2008), Int. J. Mod. Phys. A 30, 1530022 (2015)

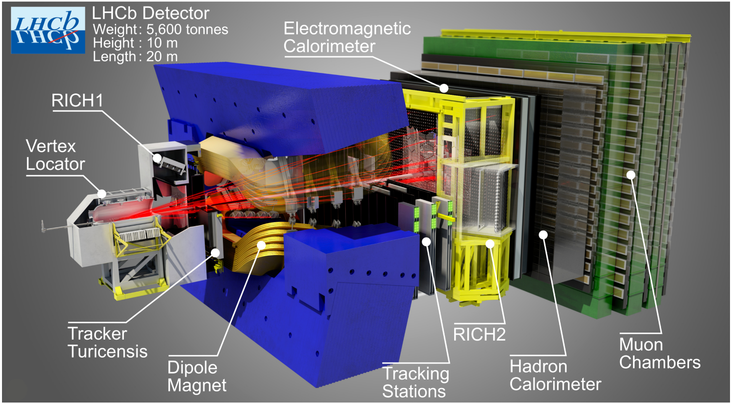

- VELO: primary and secondary vertex
- Tracking: momentum of charged particle
- RICHs: particle identification $K^{\pm}$, $\pi^{\pm}$
- MUON: trigger on high p_{T} $\mu^{\pm}$ & PID
- Calorimeter: ECAL and HCAL for γ, $e^{\pm}$ and hadronic energy

Measurement strategy

differential production cross-section in each (p_{T}, y) bin

$$\frac{\mathrm{d}^2\sigma}{\mathrm{d}y\mathrm{d}p_{\mathrm{T}}} = \frac{N(H\to f)}{L_{\text{int}}\times\epsilon_{\text{tot}}(H\to f)\times\mathcal{B}(H\to f)\times\Delta y\times\Delta p_{\mathrm{T}}}$$

- N($H \to f$): signal yield in each bin
- L_{int}: the integrated luminosity
- $\epsilon_{\text{tot}}(H \to f)$: total efficiency
- $\mathcal{B}$: the absolute branching fraction of the reconstructed initial state hadron H into its final state f
- Δy and Δp_{T} are the rapidity and p_{T} bin widths

Λ_b^0 and $\bar{B}^0$ production at $\sqrt{s} = 7$ and 8 TeV

arXiv:1509.00292

- $L_{\text{int}} = 3\,\text{fb}^{-1}$
- measure $\mathcal{B} \times \frac{\mathrm{d}^2\sigma}{\mathrm{d}y\mathrm{d}p_T}$ using decays $\Lambda_b^0 \to \mathrm{J}/\psi p K^-$ and $\overline{B}^0 \to \mathrm{J}/\psi \overline{K}^*(892)^0$
- kinematic range: $p_{\mathrm{T}} < 20\ \mathrm{GeV}/c$, $2<y<4.5$ of b-hadron
- branching fractions including $\overline{B}^0 \to \mathrm{J}/\psi \overline{K}^{*0}$ and $f_{\Lambda_b^0}/f_d$:

$$\mathcal{B}(\Lambda_b^0 \to \mathrm{J}/\psi p K^-) = (3.04 \pm 0.04 \pm 0.06 \pm 0.33^{+0.43}_{-0.27}) \times 10^{-5}$$
$$\mathcal{B}(\Lambda_b^0 \to \mathrm{J}/\psi p \pi^-) = (2.51 \pm 0.08 \pm 0.13^{+0.45}_{-0.35}) \times 10^{-5}$$

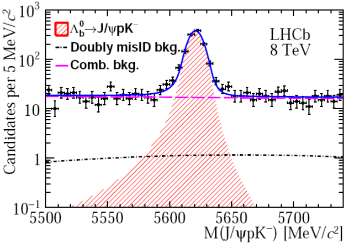

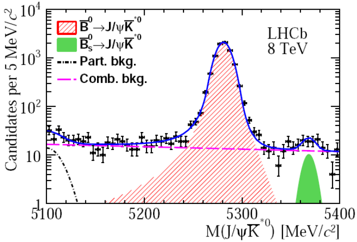

Λ_b^0 and $\bar{B}^0$ production at $\sqrt{s} = 7$ and $8\ \mathrm{TeV}$

arXiv:1509.00292

double-differential cross-section

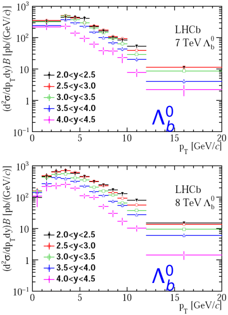

ratios between 8 and 7 TeV results

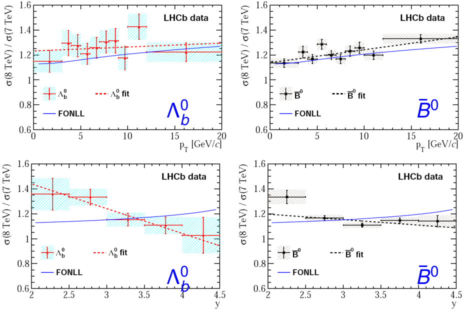

compared to FONLL predictions
(Cacciari et al., JHEP 05 (1998) 007, JHEP 03 (2001) 006, JHEP 10 (2012) 137)

integrated cross-sections

$$\sigma(\Lambda_b^0,\ \sqrt{s} = 7\,\mathrm{TeV})\ \mathcal{B}(\Lambda_b^0 \to J/\psi\, pK^-) = 6.12 \pm 0.10\,(\mathrm{stat}) \pm 0.25\,(\mathrm{syst})\,\mathrm{nb},$$
$$\sigma(\Lambda_b^0,\ \sqrt{s} = 8\,\mathrm{TeV})\ \mathcal{B}(\Lambda_b^0 \to J/\psi\, pK^-) = 7.51 \pm 0.08\,(\mathrm{stat}) \pm 0.31\,(\mathrm{syst})\,\mathrm{nb},$$
$$\sigma(\overline{B}^0,\ \sqrt{s} = 7\,\mathrm{TeV})\ \mathcal{B}(\overline{B}^0 \to J/\psi\, \overline{K}^{*0}) = 55.6 \pm 0.3\ \ (\mathrm{stat}) \pm 2.1\ \ (\mathrm{syst})\,\mathrm{nb},$$
$$\sigma(\overline{B}^0,\ \sqrt{s} = 8\,\mathrm{TeV})\ \mathcal{B}(\overline{B}^0 \to J/\psi\, \overline{K}^{*0}) = 66.2 \pm 0.3\ \ (\mathrm{stat}) \pm 2.3\ \ (\mathrm{syst})\,\mathrm{nb}.$$

Υ production at $\sqrt{s} = 7$ and 8 TeV

arXiv:1509.02372

- update of previous analyses (Eur. Phys. J. C72 (2012) 2025, JHEP 06 (2013) 064) with full statistic
- $L_{\text{int}} = 1\,\text{fb}^{-1}(7\ \text{TeV}), 2\,\text{fb}^{-1}(8\ \text{TeV}) \rightarrow$ extended kinematic range: Υ p_{T} < 30 GeV/c, 2<y<4.5
- measure $\mathcal{B}_{\Upsilon} \times \frac{\text{d}^2}{\text{d}y\text{d}p_T}\sigma(pp \rightarrow \Upsilon X)$
- extended maximum likelihood fit to invariant mass within 8.5< $m_{\mu^+\mu^-}$ <12.5 GeV/c^2 in each bin

	$\sqrt{s} = 7\,\text{TeV}$	$\sqrt{s} = 8\,\text{TeV}$
$N_{\Upsilon(1S)\to\mu^+\mu^-}$	$(2639.8 \pm 3.7) \cdot 10^3$	$(6563.1 \pm 6.3) \cdot 10^3$
$N_{\Upsilon(2S)\to\mu^+\mu^-}$	$(667.3 \pm 2.2) \cdot 10^3$	$(1674.3 \pm 3.5) \cdot 10^3$
$N_{\Upsilon(3S)\to\mu^+\mu^-}$	$(328.8 \pm 1.5) \cdot 10^3$	$(786.6 \pm 2.6) \cdot 10^3$

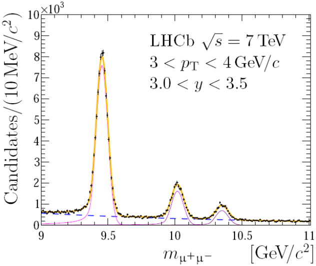

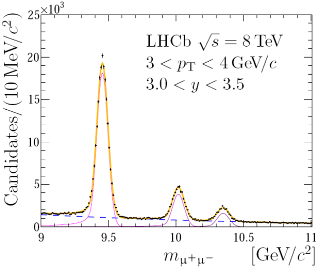

Υ production at $\sqrt{s} = 7$ and $8\ \mathrm{TeV}$

arXiv:1509.02372

double-differential cross-section for $\Upsilon(1S)$
others given in backup

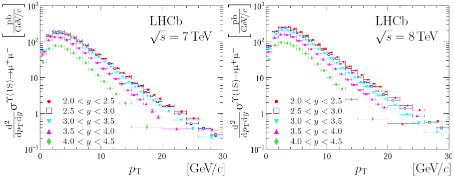

ratios between 8 and 7 TeV results

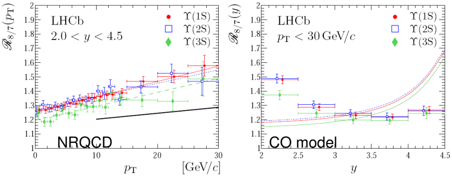

total cross-section in LHCb acceptance (in pb):

	$\sqrt{s} = 7\,\mathrm{TeV}$	$\sqrt{s} = 8\,\mathrm{TeV}$
$\sigma^{\Upsilon(1S)\to\mu^+\mu^-}$	$2510 \pm 3 \pm 80$	$3280 \pm 3 \pm 100$
$\sigma^{\Upsilon(2S)\to\mu^+\mu^-}$	$635 \pm 2 \pm 20$	$837 \pm 2 \pm 25$
$\sigma^{\Upsilon(3S)\to\mu^+\mu^-}$	$313 \pm 2 \pm 10$	$393 \pm 1 \pm 12$

- p_{T} compared to NRQCD predictions (H. Han et al. arXiv:1410.8537)
- y compared to CO model $\Upsilon(1S)$,$\Upsilon(2S)$, $\Upsilon(3S)$ (L. S. Kisslinger et al., Mod. Phys. Lett. A28 (2013) 1350120, Mod. Phys. Lett. A29 (2014) 1450082)
- increase of bottomonium production of 30% from $\sqrt{s}$=7 to 8 TeV

LHCb Run-II Trigger

- software trigger optimised for Run-II
- offline quality alignment and calibration done in quasi real-time before 2nd stage of trigger level

Turbo Stream

→ 20% of total rate

→ offline-quality analysis directly out of trigger

→ no offline reprocessing needed → very fast

→ **only saves information of selected candidates**
→ **reduced event size, increased efficiency**

→ ideal for high signal yield analysis

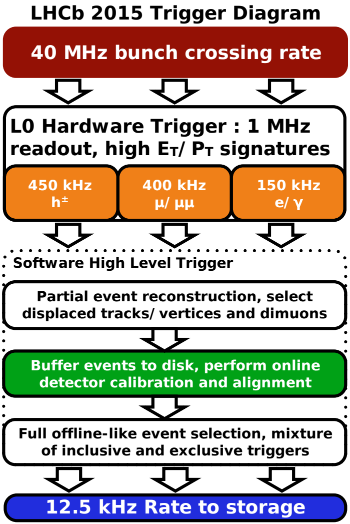

J/ψ production at $\sqrt{s} = 13$ TeV

arXiv:1509.00771

- $L_{\text{int}} = 3.05 \pm 0.12\,\text{pb}^{-1}$
- using $J/\psi \to \mu^+\mu^-$ decays
- kinematic range: $p_{\rm T}$ <14 GeV/c, 2<y<4.5
- separate prompt and J/ψ-from-b decays using pseudo decay-time $t_z = \frac{(z_{J/\psi} - z_{PV}) \times M_{J/\psi}}{p_z}$

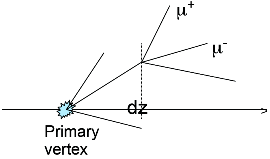

- unbinned extended maximum likelihood fit in mass and t_z

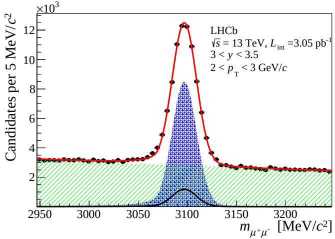

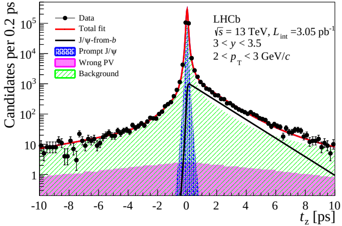

J/ψ production at $\sqrt{s} = 13$ TeV

arXiv:1509.00771

prompt J/ψ

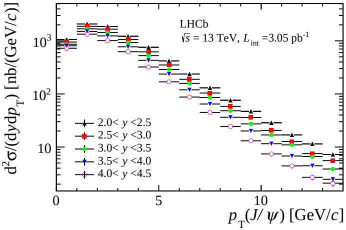

J/ψ-from-*b*

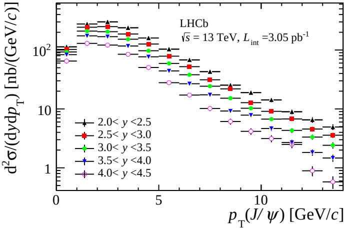

b-fraction

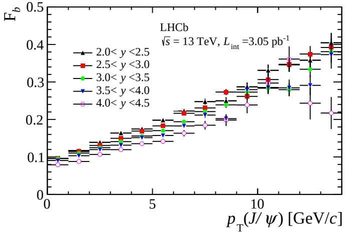

integrated cross-section in LHCb acceptance

$\sigma(\text{prompt}) = 15.40 \pm 0.03(\text{stat}) \pm 0.86(\text{syst})\ \mu\text{b}$
$\sigma(J/\psi\text{-from-}b) = 2.36 \pm 0.01(\text{stat}) \pm 0.13(\text{syst})\ \mu\text{b}$

$b\bar{b}$ cross-section with 4π extrapolation*

$\sigma(b\bar{b}) = 519 \pm 2(\text{stat}) \pm 53(\text{syst})\ \mu\text{b}$

*'naive' extrapolation factor using LHCb tuning of PYTHIA 6

J/ψ production at $\sqrt{s} = 13$ TeV

arXiv:1509.00771

comparison with theory

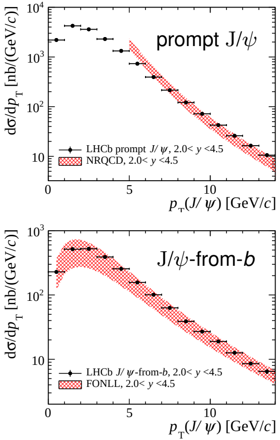

cross-section ratio

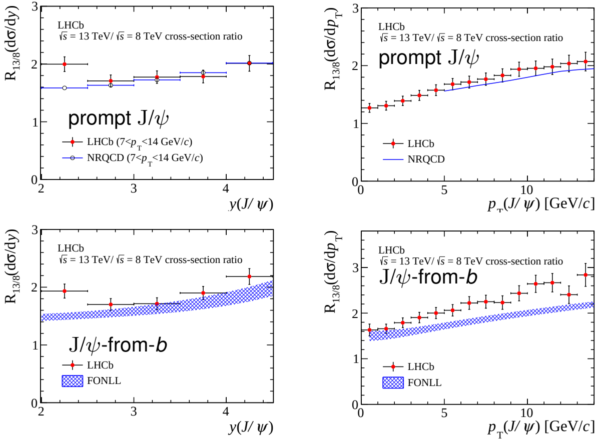

NRQCD (Shao et al., JHEP 05 (2015) 103), FONLL (Cacciari et al., JHEP 05 (1998) 007,Cacciari et al., arXiv:1507.06197)

prompt charm production at $\sqrt{s} = 13\ \mathrm{TeV}$

LHCb-PAPER-2015-041

- $L_{\mathrm{int}} = 4.98 \pm 0.19\,\mathrm{pb}^{-1}$
- use charm decays: $D^0 \to K^-\pi^+$, $D^+ \to K^-\pi^+\pi^+$, $D_s^+ \to K^-K^+\pi^+$, $D^{*+} \to D^0\pi^+$ (here only D^0 others given in backup)
- kinematic range: $p_{\mathrm{T}} < 15\ \mathrm{GeV}/c$, 2<y<4.5
- separate prompt from secondary signal using impact parameter (IP) significance

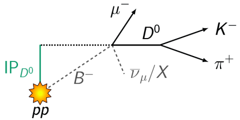

- candidates selected in mass window around nominal charm hadron mass
- signal yield extracted from fit to $\log(\chi^2_{IP})$ in each bin

Hadron	Prompt signal yield
D^0	$(2.577 \pm 0.002) \times 10^6$
D^+	$(1.974 \pm 0.002) \times 10^6$
D_s^+	$(1.13 \pm 0.4) \times 10^5$
D^{*+}	$(3.01 \pm 0.6) \times 10^5$

$D^0 \to K^-\pi^+$

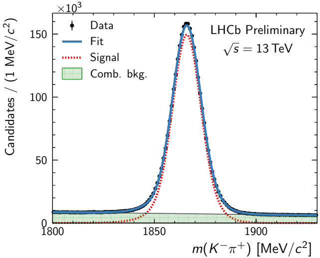

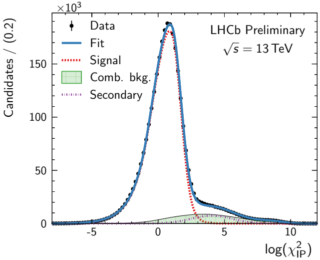

prompt charm production at $\sqrt{s} = 13\ \mathrm{TeV}$

LHCb-PAPER-2015-041

double-differential cross-section $D^0 \to K^-\pi^+$

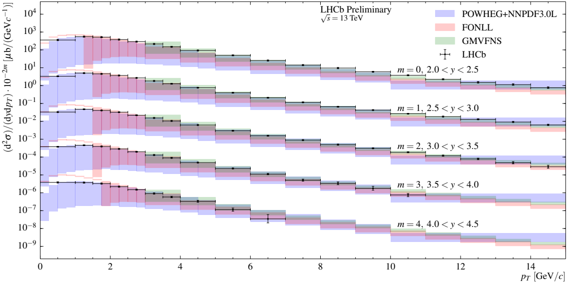

cross-section ratio $D^0 \to K^-\pi^+$

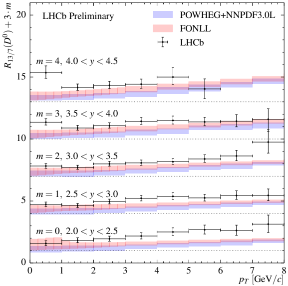

compare to theory predictions:

- POWHEG+NNPDF3.0L (Gauld et al., arXiv:1506.08025)
- FONLL (Cacciari et al.,arXiv:1507.06197)
- General-mass variable-flavor-number (GMVFNS) (Spiesberger et al., arXiv:1202.0439)

- good agreement with theory predictions of shape
- central value lies consistently above calculations, agree within uncertainties

prompt charm production at $\sqrt{s} = 13\ \mathrm{TeV}$

LHCb-PAPER-2015-041

integrated cross-section $\sigma(c\bar{c})$

- calculated in region $0 < p_{\mathrm{T}} < 8\ \mathrm{GeV}/c$, $2 < y < 4.5$
- use integrated D^0 and D^+ cross-sections
- combined with fragmentation fractions $f(c \to H_c)$ from e^+e^- colliders (C. Amsler et al., doi:10.1016/j.physletb.2008.07.018.)
- extrapolate into bins with no measurements using theory predictions

$\sigma(c\bar{c})$ production cross-section

$$\sigma(c\bar{c}) = 2850 \pm 3(\text{stat}) \pm 180(\text{syst}) \pm 144(\text{frag})\ \mu\mathrm{b}$$

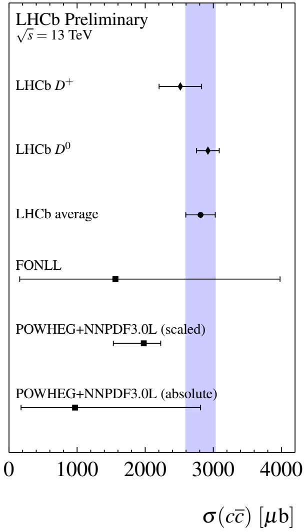

Conclusions

- selection of recent production measurement from **Run-I** by LHCb shown

- first **Run-II** results on production measurements are ready
  - **thanks to the excellent detector performance and new trigger strategy**

    $\rightarrow$ allows for quick results:
    - J/ψ cross-section is submitted to JHEP (arXiv:1509.00771)
    - prompt charm cross-section will be released soon LHCb-PAPER-2015-041

- agreement with theory predictions is reasonable, some tension in the cross-section ratio measurements

more analyses are in the pipeline, stay tuned!

Thanks for your attention!

Backup Slides

LHCb Trigger in Run-I

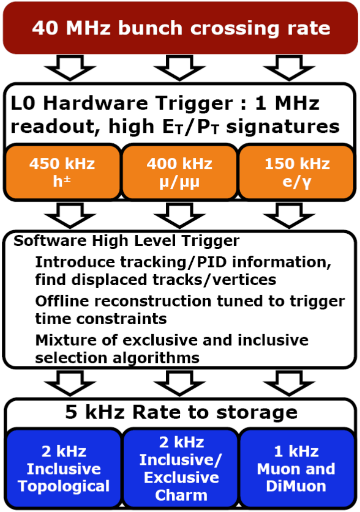

Λ_b^0 and $\bar{B}^0$ production at $\sqrt{s} = 7$ and $8\ \mathrm{TeV}$

systematic uncertainties:

arXiv:1509.00292

	Λ_b^0 (7 TeV)	Λ_b^0 (8 TeV)	$\overline{B}^0$ (7 TeV)	$\overline{B}^0$ (8 TeV)
Uncorrelated between bins				
Signal shape	0.4 – 15.4	0.2 – 6.2	0.2 – 1.5	0.2 – 1.5
Background shape	0.0 – 1.9	0.0 – 4.3	0.0 – 0.9	0.0 – 0.9
Simulation sample size	4.1 – 16.5	3.9 – 14.3	1.7 – 9.5	2.2 – 14.9
BDT efficiency	0.4 – 2.5	0.4 – 2.8	0.1 – 0.5	0.1 – 0.5
Trigger efficiency	0.0 – 4.6	0.0 – 14.9	0.0 – 2.1	0.0 – 4.0
PID efficiency	0.4 – 8.4	0.4 – 15.8	0.2 – 4.6	0.2 – 2.7
Resonance in $\Lambda_b^0 \to J/\psi\, pK^-$	0.1 – 7.7	0.4 – 2.4		
Correlated between bins				
Tracking efficiency	3.0	3.0	3.0	3.0
Mass veto efficiency	1.3	1.9		
Luminosity	1.7	1.2	1.7	1.2
$\mathcal{B}(J/\psi \to \mu^+\mu^-)$	0.6	0.6	0.6	0.6
S-wave in $K^-\pi^+$			1.1	1.1

Λ_b^0 and $\bar{B}^0$ production at $\sqrt{s} = 7$ and 8 TeV

arXiv:1509.00292

- mis-identified bkg from $\overline{B}^0 \to J/\psi K^- \pi^+$ and $\overline{B}_s^0 \to J/\psi K^- K^+$ reduced using mass-vetoes
- $\overline{K}^{*0} \to K^- \pi^+$ s-wave contribution is subtracted

integrated cross sections

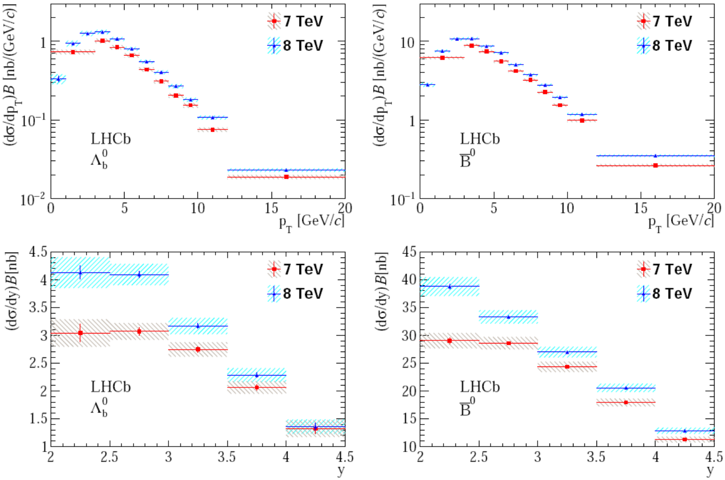

Λ_b^0 and $\bar{B}^0$ production at $\sqrt{s} = 7$ and $8\ \mathrm{TeV}$

arXiv:1509.00292

branching fraction results

$$R_{\Lambda_b^0/\bar{B}^0}(p_{\mathrm{T}}) = \frac{N_{\mathrm{sig}}^{\Lambda_b^0}(p_{\mathrm{T}})\ \varepsilon_{\mathrm{tot}}^{\bar{B}^0}(p_{\mathrm{T}})}{N_{\mathrm{sig}}^{\bar{B}^0}(p_{\mathrm{T}})\ \varepsilon_{\mathrm{tot}}^{\Lambda_b^0}(p_{\mathrm{T}})}\ \mathcal{B}(\overline{K}^{*0} \to K^-\pi^+)$$

can be related to $f_{\Lambda_b^0}/f_d$ through

$$R_{\Lambda_b^0/\bar{B}^0}(p_{\mathrm{T}}) = \frac{\mathcal{B}(\Lambda_b^0 \to J/\psi\, pK^-)}{\mathcal{B}(\overline{B}^0 \to J/\psi\, \overline{K}^{*0})} f_{\Lambda_b^0}/f_d(p_{\mathrm{T}}) \equiv \mathcal{S}\ f_{\Lambda_b^0}/f_d(p_{\mathrm{T}})$$

with S as a constant factor obtained from fit, gives:

$\mathcal{B}(\Lambda_b^0 \to \mathrm{J}/\psi pK^-) = (3.04 \pm 0.04 \pm 0.06 \pm 0.33^{+0.43}_{-0.27}) \times 10^{-5}$

together with the ratio $\mathcal{B}(\Lambda_b^0 \to \mathrm{J}/\psi pK^-)/\mathcal{B}(\Lambda_b^0 \to \mathrm{J}/\psi p\pi^-)$ measured in JHEP 07 (2014) 103 it gives:

$\mathcal{B}(\Lambda_b^0 \to \mathrm{J}/\psi p\pi^-) = (2.51 \pm 0.08 \pm 0.13^{+0.45}_{-0.35}) \times 10^{-5}$

with the fraction of Pentaquarks observed in $m(\mathrm{J}/\psi p)$ (Phys. Rev. Lett. 115 (2015) 072001, see Zhenwei's talk), gives the branching ratio:

$$\mathcal{B}(\Lambda_b^0 \to P_c^+ K^-)\mathcal{B}(P_c^+ \to \mathrm{J}/\psi p) = \begin{cases} (2.56 \pm 0.22 \pm 1.28^{+0.46}_{-0.36}) \times 10^{-5} & \text{for } P_c(4380)^+ \\ (1.25 \pm 0.15 \pm 0.33^{+0.22}_{-0.18}) \times 10^{-5} & \text{for } P_c(4450)^+ \end{cases}$$

Λ_b^0 and $\bar{B}^0$ production at $\sqrt{s} = 7$ and 8 TeV

arXiv:1509.00292

fit with power-law function with Tsallis parametrisations:

$$\frac{\mathrm{d}\sigma}{p_\mathrm{T}\mathrm{d}p_\mathrm{T}} \propto \frac{1}{[1 + E_{k\perp}/(TN)]^N} \text{ with } E_{k\perp} \equiv \sqrt{{p_\mathrm{T}}^2 + M^2} - M$$

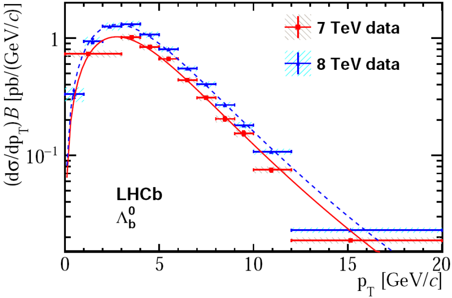

fit results give $T = 1.12 \pm 0.04(1.13 \pm 0.03)$ GeV and $N = 7.3 \pm 0.5(7.5 \pm 0.4)$ at 7(8) TeV and are consistent with results from CMS

Λ_b^0 and $\bar{B}^0$ production at $\sqrt{s} = 7$ and 8 TeV

arXiv:1509.00292

kinematic dependence of the sum of the asymmetries in production and decays ($a_{p+d} \equiv a_{prod} + a_{decay}$) of Λ_b^0 and $\overline{\Lambda}_b^0$ is studied:

$a_{p+d}(x) = A_{raw}(x) - a_{PID}(x) - a_D^p(x) - a_D^K(x)$

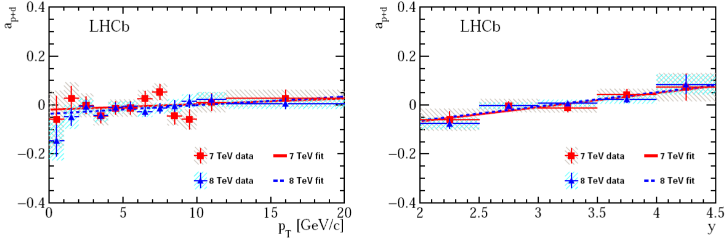

data points are fitted with linear function, slope as function of $p_{\rm T}$ consistent with zero

slope of $a_{p+d}(y) = (-0.001 \pm 0.007) + (0.058 \pm 0.014)(y - \langle y \rangle)$ with $\langle y \rangle = 3.1$ is the average rapidity of Λ_b^0

$\rightarrow$ suggests baryon number transport from beam particles to less central produced Λ_b^0, interpreted by string drag effect or leading quark effect (Phys. Rev. D90 (2014) 014023, Phys. Rev. D86 (2012) 014011)

Λ_b^0 and $\bar{B}^0$ production at $\sqrt{s} = 7$ and $8\ \mathrm{TeV}$

arXiv:1509.00292

measure also ratio: $R_{\Lambda_b^0/\bar{B}^0} \equiv \dfrac{\sigma(\Lambda_b^0)\mathcal{B}(\Lambda_b^0 \to \mathrm{J}/\psi p K^-)}{\sigma(\overline{B}^0)\mathcal{B}(\overline{B}^0 \to \mathrm{J}/\psi \overline{K}^{*0})}$

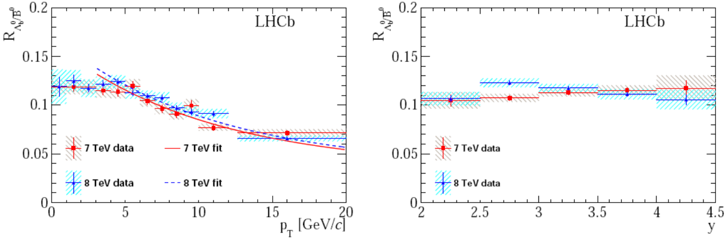

it decreases for $p_{\mathrm{T}} > 5\ \mathrm{GeV}/c$, fitted with fragmentation function ratio $f_{\Lambda_b^0}/f_d(p_{\mathrm{T}})$ for $p_{\mathrm{T}} > 3\ \mathrm{GeV}/c$

systematic uncertainties:

	2011	2012
PID efficiency	0.4 – 4.4	0.0 – 2.6
Signal shape	0.0 – 0.8	0.0 – 0.9
Background shape	0.0 – 0.1	0.0 – 0.3
MC statistics	0.7 – 5.4	0.3 – 4.2
Tracking asymmetry of proton	0.1 – 1.9	0.1 – 1.9

Υ production at $\sqrt{s} = 7$ and 8 TeV

arXiv:1509.02372

systematic uncertainties:

Table 2: Summary of relative systematic uncertainties (in %) for the differential production cross-sections, their ratios, integrated cross-sections and the ratios $\mathscr{R}_{8/7}$. The ranges indicate variations depending on the (p_{T}, y) bin and the Υ state.

Source	$\sigma_{\mathrm{bin}}^{\Upsilon\to\mu^+\mu^-}$	$\mathscr{R}_{\mathrm{i,j}}$	$\sigma^{\Upsilon\to\mu^+\mu^-}$	$\mathscr{R}_{8/7}$
Fit model and range	$0.1 - 4.8$	$0.1 - 2.9$	0.1	—
Efficiency correction	$0.2 - 0.6$	$0.1 - 1.1$	0.4	—
Efficiency uncertainty	$0.2 - 0.3$	—	0.2	0.3
Muon identification	$0.3 - 0.5$	—	0.3	0.2
Data-simulation agreement				
Radiative tails	1.0	—	1.0	—
Selection efficiency	1.0	0.5	1.0	0.5
Tracking efficiency	$0.5 \oplus (2 \times 0.4)$	—	$0.5 \oplus (2 \times 0.4)$	—
Trigger efficiency	2.0	—	2.0	1.0
Luminosity	$1.7\,(\sqrt{s} = 7\,\mathrm{TeV})$ $1.2\,(\sqrt{s} = 8\,\mathrm{TeV})$	—	$1.7\,(\sqrt{s} = 7\,\mathrm{TeV})$ $1.2\,(\sqrt{s} = 8\,\mathrm{TeV})$	1.4

Υ production at $\sqrt{s} = 7$ and 8 TeV

arXiv:1509.02372

$\Upsilon(1S)$

$\Upsilon(2S)$

$\Upsilon(3S)$

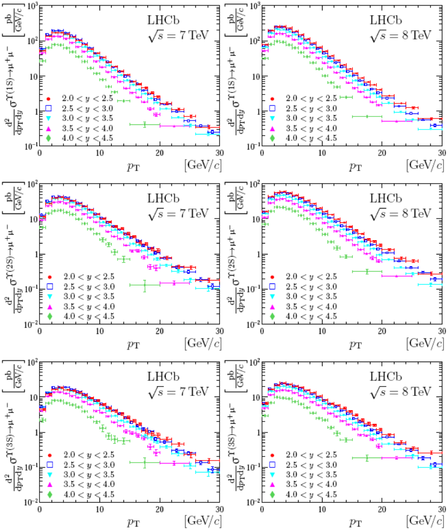

double-differential production cross-sections

Υ production at $\sqrt{s} = 7$ and 8 TeV

arXiv:1509.02372

fit with Tsallis function with power law behaviour for large p_T

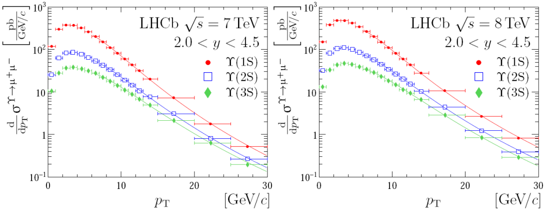

fit gives N 8 consistent with high p_T asymptotic behaviour from CS model, T increases with mass of Υ state

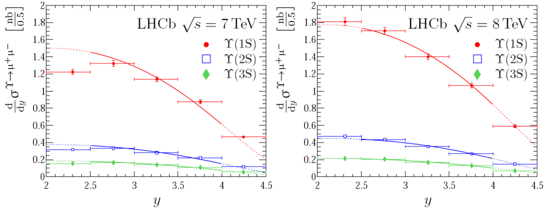

shape of rapidity compared to CM model

Υ production at $\sqrt{s} = 7$ and 8 TeV

arXiv:1509.02372

$$\mathscr{R}_{i,j} \equiv \frac{\sigma_{\text{bin}}^{\Upsilon(iS)\to\mu^+\mu^-}}{\sigma_{\text{bin}}^{\Upsilon(jS)\to\mu^+\mu^-}} = \frac{N_{\Upsilon(iS)\to\mu^+\mu^-}}{N_{\Upsilon(jS)\to\mu^+\mu^-}}$$

production ratios of various Υ mesons

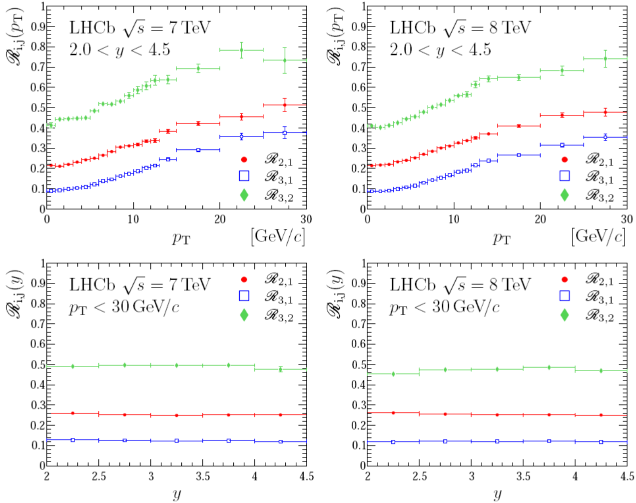

J/ψ production at $\sqrt{s} = 13\ \mathrm{TeV}$

arXiv:1509.00771

details on included theoretical uncertainties in ratios:

- **NRQCD**: includes CO LDME uncertainties which are dominant for the absolute measurement, not included here are contributions from renormalization/factorization scale, relativistic corrections, charm mass uncertainty and PDF uncertainty
  almost cancel in ratio
- **FONLL**: b-quark mass, renormalisation and factorisation scales, for ratio also gluon PDF uncertainty included

J/ψ production at $\sqrt{s} = 13$ TeV

arXiv:1509.00771

Systematic uncertainties

Table 1: Relative systematic uncertainties (in %) on the J/ψ cross-section measurements. The uncertainty from the t_z fit only affects J/ψ-from-b mesons. Most of the uncertainties are fully correlated between bins, with the exception of the p_{T}, y spectrum dependence and the simulation statistics, which are considered uncorrelated.

Source	Systematic uncertainty (%)
Luminosity	3.9
Hardware trigger	0.1 – 5.9
Software trigger	1.5
Muon ID	1.8
Tracking	1.1 – 3.4
Radiative tail	1.0
J/ψ vertex fit	0.4
Signal mass shape	1.0
$\mathcal{B}(J/\psi \to \mu^+\mu^-)$	0.6
p_{T}, y spectrum	0.1 – 5.0
Simulation statistics	0.3 – 5.0
t_z fit (J/ψ-from-b only)	0.1

J/ψ production at $\sqrt{s} = 13$ TeV

arXiv:1509.00771

comparison with $\sqrt{s} = 8$ TeV results

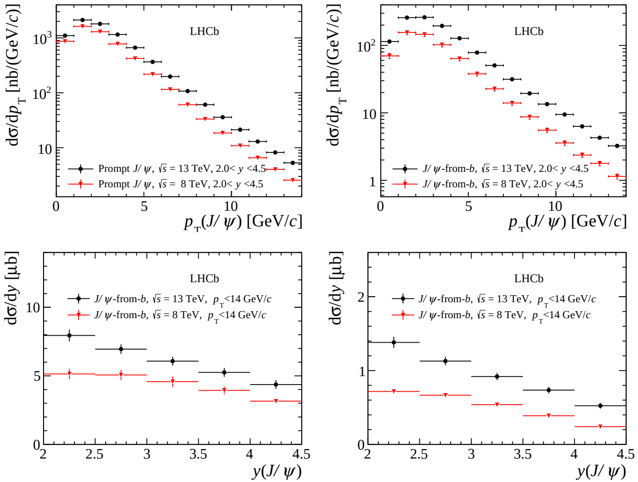

J/ψ production at $\sqrt{s} = 13$ TeV

arXiv:1509.00771

cross-section as function of $\sqrt{s}$

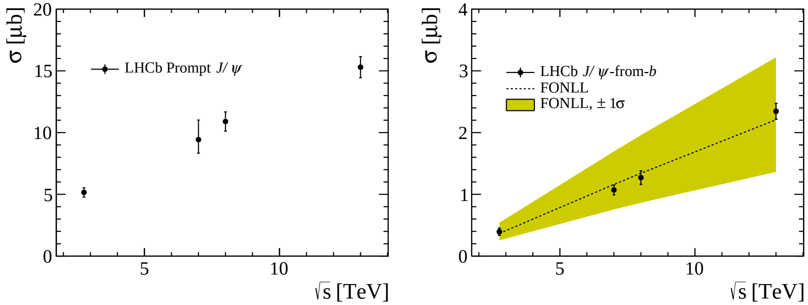

compared with FONLL predictions (Cacciari et al., JHEP 9805 (1998) 007)

prompt charm production at $\sqrt{s} = 13\ \mathrm{TeV}$

LHCb-PAPER-2015-041

Systematic uncertainties

Table 2: Overview of systematic uncertainties and their values, expressed as relative fractions of the cross-section measurements in percent. Uncertainties that are computed bin-by-bin are expressed as ranges giving the minimum to maximum values of the bin uncertainties. Ranges for the correlations between p_T-y bins and between modes are given, expressed in percent.

	D^0	D^+	D_s^+	D^{*+}	Bins	Modes
Luminosity	3.9				100	100
Tracking	3–5	5–11	4–11	5–12	90–100	90–100
Branching fractions	1.2	2.1	4.5	1.5	100	0–95
MC sample size	2-50	1-50	3-180	2-170	-	-
MC modelling	2	1	1	1	-	-
PID sample size	0–1	0–1	0–1	0–1	0–100	-
PID binning	0–42	0–11	0–18	0-15	100	100
Fit shapes	1–3	1–3	1–2	1–2	-	-

prompt charm production at $\sqrt{s} = 13\ \mathrm{TeV}$

LHCb-PAPER-2015-041

double-differential cross-section $D^+ \to K^-\pi^+\pi^+$

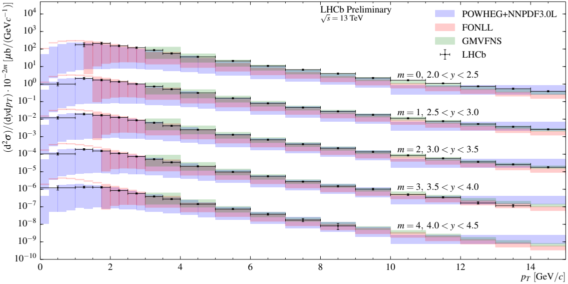

cross-section ratio $D^+ \to K^-\pi^+\pi^+$

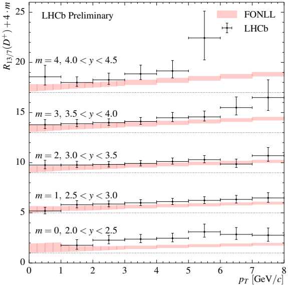

compare to theory predictions:

- POWHEG+NNPDF3.0L (Gauld et al., arXiv:1506.08025)
- FONLL (Cacciari et al.,arXiv:1507.06197)
- General-mass variable-flavor-number (GMVFNS) (Spiesberger et al., arXiv:1202.0439)

- good agreement with theory predictions
- data lies consistently above calculations

prompt charm production at $\sqrt{s} = 13\ \mathrm{TeV}$

LHCb-PAPER-2015-041

double-differential cross-section $D_s^+ \to K^- K^+ \pi^+$

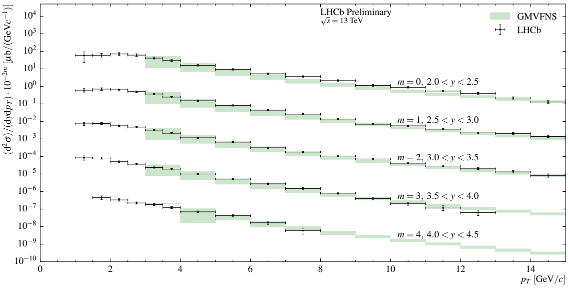

cross-section ratio $D_s^+ \to K^- K^+ \pi^+$

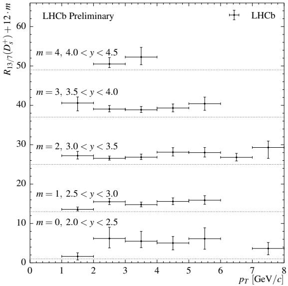

compare to theory predictions:

- POWHEG+NNPDF3.0L (Gauld et al., arXiv:1506.08025)
- FONLL (Cacciari et al.,arXiv:1507.06197)
- General-mass variable-flavor-number (GMVFNS) (Spiesberger et al., arXiv:1202.0439)

- good agreement with theory predictions
- data lies consistently above calculations

prompt charm production at $\sqrt{s} = 13\ \mathrm{TeV}$

LHCb-PAPER-2015-041

double-differential cross-section $D^{*+} \to D^0\pi^+$

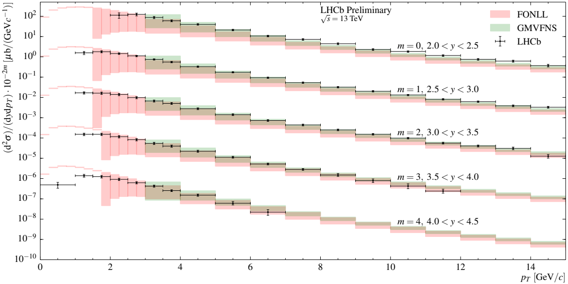

cross-section ratio $D^{*+} \to D^0\pi^+$

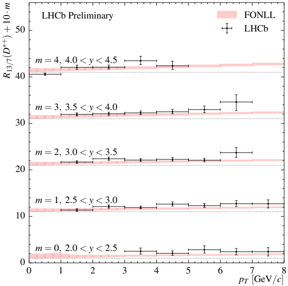

compare to theory predictions:

- POWHEG+NNPDF3.0L (Gauld et al., arXiv:1506.08025)
- FONLL (Cacciari et al.,arXiv:1507.06197)
- General-mass variable-flavor-number (GMVFNS) (Spiesberger et al., arXiv:1202.0439)

- good agreement with theory predictions
- data lies consistently above calculations

prompt charm production at $\sqrt{s} = 13\ \mathrm{TeV}$

LHCb-PAPER-2015-041

details on included theoretical uncertainties:
all performed @NLO precision

- **POWHEG+NNPDF3.0L**: include factorisation, renormalisation scale, charm quark mass and PDF uncertainties
  obtained with POWHEG matched to Pythia8 parton showers and an improved version of the NNPDF3.0 NLO parton distribution function set designated NNPDF3.0+LHCb. To produce this improved set, the authors weight the NNPDF3.0 NLO set in order to match FONLL calculations to LHCb's charm cross-section measurements at 7TeV. This results in a significant improvement in the uncertainties for the gluon distribution function at small Bjorken-x.
- **FONLL**: include factorisation, renormalisation scale, charm quark mass and PDF uncertainties, uses NNPDF3.0 NLO parton densities, assume unit transition probabilities from a primary charm quark to the exclusive hadron state
- **General-mass variable-flavor-number (GMVFNS)**: include factorisation and renormalisation scale uncertainties
  Here the CT10 set of parton distributions was used. The GMVFNS theoretical framework includes the convolution with fragmentation functions describing the transition c $\rightarrow H_c$ that are normalised to the respective total transition probabilities. The fragmentation functions are results of a fit to production measurements at e+e- colliders, where no attempt was made in the fit to separate direct production and feed-down from higher resonances.